Binding, Internalization, and Lysosomal Association of ^{125}I-Glucagon in Isolated Rat Hepatocytes

A QUANTITATIVE ELECTRON MICROSCOPE AUTORADIOGRAPHIC STUDY

PHILIPPE BARAZZONE, PHILLIP GORDEN, JEAN-LOUIS CARPENTIER, and LELIO ORCI, *Institute of Histology and Embryology, University of Geneva Medical School, Geneva, Switzerland*

PIERRE FREYCHET and BERTRAND CANIVET, *Institut National de la Santé et de la Recherche Medicale, Department of Experimental Medicine, Nice, France*

ABSTRACT When ^{125}I-glucagon is incubated with freshly isolated rat hepatocytes and studied by quantitative electron microscope autoradiography, the labeled material localizes to the plasma membrane of the cell at early times of incubation at 20°C; at later times of incubation at 20°C, there is little further translocation of the labeled ligand. When incubations are carried out at 37°C, the labeled material is progressively internalized by the cell after a brief delay. When the internalized radioactivity is further analyzed, it is found to associate preferentially with lysosome-like structures. When the cell-associated radioactivity is extracted, there is degradation of the ligand in incubations carried out at 37°C.

The events involved in the interaction of ^{125}I-glucagon with the hepatocyte are similar to those previously described for labeled insulin in this cell. The process of binding, internalization, and lysosomal association appears to be a general process related to many polypeptide hormones and growth factors, and may represent the mechanism by which the specific binding of the ligand to the cell surface mediates the degradation of the ligand and the loss of its surface receptor.

INTRODUCTION

Glucagon is a polypeptide hormone secreted by the A cell of the islets of Langerhans and gastrointestinal tract that plays an important role in fuel homeostasis. The hormone produces these metabolic effects by activating the enzyme adenylate cyclase to form cyclic 3′5′-AMP, which in turn activates a series of phosphorylation steps (1–3). The essential components of this system, i.e., the receptor, the catalytic component, and other regulatory components, are contained in the plasma membrane; and glucagon is a classic example of a polypeptide hormone that activates a second messenger (3).

It has been demonstrated recently by quantitative electron microscope (EM)[1] autoradiography in rat hepatocytes in vitro and in rat liver in vivo that ^{125}I-insulin binds to the plasma membrane of the hepatocyte and is subsequently internalized by the cell (4–8). Insulin, in contrast to glucagon, has no known second messenger and the mechanism involved in its activation of intracellular processes is unknown.

In this investigation we have studied the morphologic events involved in the interaction of ^{125}I-glucagon with freshly isolated rat hepatocytes and have compared these events with insulin and other polypeptide hormones.

METHODS

Cells and reagents. Hepatocytes were isolated from 6–8-wk-old male Wistar rats fed ad lib. by a modification of the method of Seglen (9). The cells were suspended in buffer, then washed four times by low-speed centrifugation. 95% of the cell suspension obtained by this procedure are hepatocytes and 85% of these hepatocytes are viable as judged by two criteria: their ability to exclude trypan blue

This work was performed while Dr. P. Gorden was visiting professor at the Institute of Histology and Embryology, University of Geneva, Switzerland.

Received for publication 17 December 1979 and in revised form 14 July 1980.

[1] *Abbreviation used in this paper*: EM, electron microscope.

and their peripheral refractoriness under the phase-contrast microscope. After 60 min at 37°C and 120 min at 20°C, the proportion of viable cells is >75%. ^{125}I-Glucagon was prepared at a specific activity of 68–98 μCi/μg by a modification of the chloramine T method (10), and labeled glucagon was purified by gel filtration on a Sephadex G-50 column before each experiment.

Incubation conditions. Hepatocytes (1×10^6 cells/ml) were incubated in duplicate with 0.7 nM ^{125}I-glucagon in 0.5 ml of Krebs-Ringer bicarbonate buffer (pH 7.5) containing 3% bovine serum albumin (fraction V) and bacitracin (0.8 mg/ml). Cells were incubated at 20° and 37°C for varing periods of time in plastic Falcon tubes (Falcon Labware, Div. of Becton, Dickinson & Co., Oxnard, Calif.). For each incubation time, identical incubations were carried out in the presence of 30 μM unlabeled glucagon to determine the nonspecific binding (cell-associated radioactivity in the presence of an excess of unlabeled hormone). At the end of each incubation period, 1 ml of chilled buffer was added to each tube, which was then centrifuged at 50*g* for 20 s. The supernate was removed and the cell pellet quickly resuspended in 1 ml of chilled buffer and centrifuged for 30 s at 500*g* in a Beckman plastic microfuge tube (Beckman Instruments, Inc., Spinco Div., Palo Alto, Calif.). Cell pellets were washed once more without resuspension and with chilled buffer containing sucrose (100 mg/ml). 4% glutaraldehyde in 0.1 M phosphate buffer (pH 7.4) was added to each pellet, which was allowed to fix for 2.5–4 h at room temperature. The glutaraldehyde was then aspirated and replaced with 0.1 M phosphate buffer (pH 7.4), and the radioactivity in duplicate cell pellets determined in a gamma counter.

Preparation for electron microscopy and autoradiography. Cell pellets were washed three times in phosphate buffer, postfixed in 0.1 M osmium tetroxide in phosphate buffer 0.1 M (pH 7.4), progressively dehydrated in graded ethanol, embedded in Epon (Shell Chemical Co., Houston, Tex.), cut in 60–80-nm thin sections, and placed on copper grids. The grids were coated with Ilford L4 emulsion (Ilford Ltd., Ilford, Essex, England) by the method of Caro et al. (11), incubated at 4°C for 3 wk, and developed with Microdol X (Eastman Kodak Co., Rochester, N. Y.) as previously described (12). Preparations were then stained with uranyl acetate and lead citrate and examined on a Philips EM 300 electron microscope (Philips, Eindhoven, The Netherlands).

Sampling and analysis of data. For each time point analyzed, three blocks were used, and two sections were cut from each block. Developed grains were photographed on cells judged morphologically well preserved at an initial magnification of ×10,000 calibrated with a reference grid (2,160 lines/mm). A mean of 150 consecutive grains was photographed for each time point. Grain center was determined as previously described (12), and the distance between the grain center and the closest plasma membrane was measured on positive prints at a final magnification of ×30,000. The normalized number of grains or the percent total grains was plotted as a function of the distance between the grain center and the plasma membrane (13).

Morphometry. To know if internalized grains had a preferential association with intracellular organelles, a probability circle method (14) was applied as previously described (6). We used as reference previously published morphometric data (6) of the volume density for the different structures analyzed (mitochondria, microbodies, lysosomal structures, glycogen, rough endoplasmic reticulum). The total number of points accumulated for a given organelle was then calculated and expressed as a percentage of the total number of grains counted.

Analysis of cell-associated radioactivity. In a separate set of incubations at 20° and 37°C, cells were centrifuged and washed as described under incubation conditions. the cell pellet was mixed with a solution composed of 0.1% Triton X-100, 3 M acetic acid, and 6 M urea. This mixture was centrifuged in a Beckman microfuge (Beckman Instruments Inc.) at 12,000*g* for 5 min at room temperature; 87–97% of the total cellular radioactivity was found in the supernate. The extract was then applied to a G-50 (fine) column (0.9 × 50 cm), which was equilibrated in and eluted by either the extraction mixture or by 1 M acetic acid. 1-ml samples were collected on an automated fraction collector. Aliquots of the media were taken at each time point of incubation and applied directly to the Sephadex column as above and, in addition, were examined for precipitability by trichloracetic acid and adsorption to talc.

RESULTS

General characteristics of the isolated hepatocytes. The isolated hepatocytes used for these experiments are 22.0±0.1 μm in diameter. They have the typical morphological characteristics of other isolated hepatocytes previously described (15, 16). As seen by scanning EM (Fig. 1) and in thin sections (Fig. 2), the cells are well isolated and well preserved. Biochemical studies provide evidence for the functional integrity of these cells: they are able to bind labeled insulin and glucagon (16) and to respond metabolically to catecholamines (17), glucagon (18, 19), corticosteroids (20), and insulin (21).

Quantitative studies of the initial interaction of

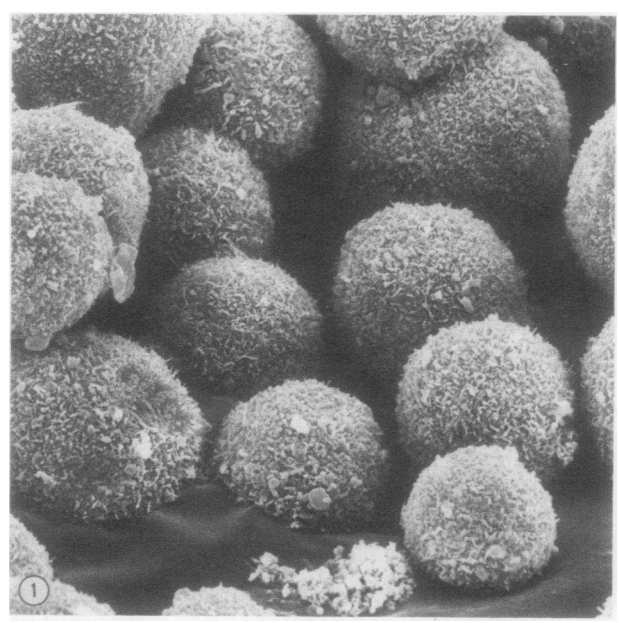

FIGURE 1 Low-power view of isolated hepatocytes. These cells have a mean diameter of 22 μm as measured in the standard incubation media, and this scanning electron micrograph illustrates their three-dimensional aspect: the cells assume a rounded shape, and their surface is covered with numerous microvilli. ×1,800.

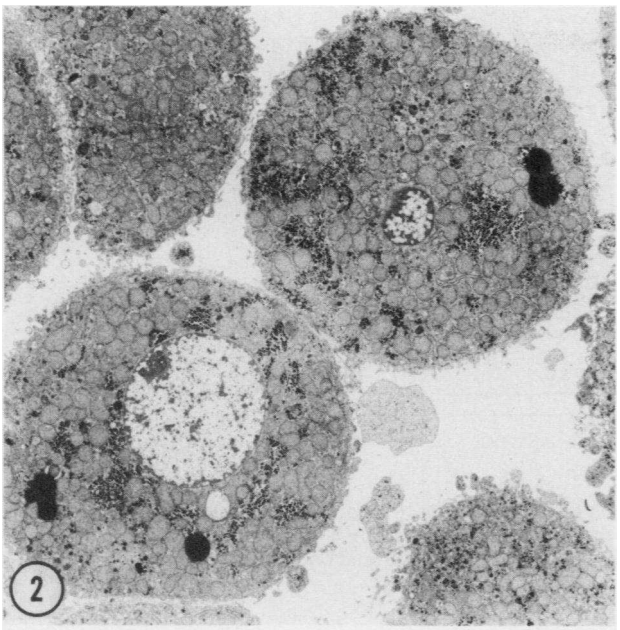

FIGURE 2 Transmission electron micrograph of a thin section of similar cells. This picture, representative of the isolated status of the cells in the various incubations studied, shows a good ultrastructural preservation of the plasma membrane and the cytoplasm. ×2,200.

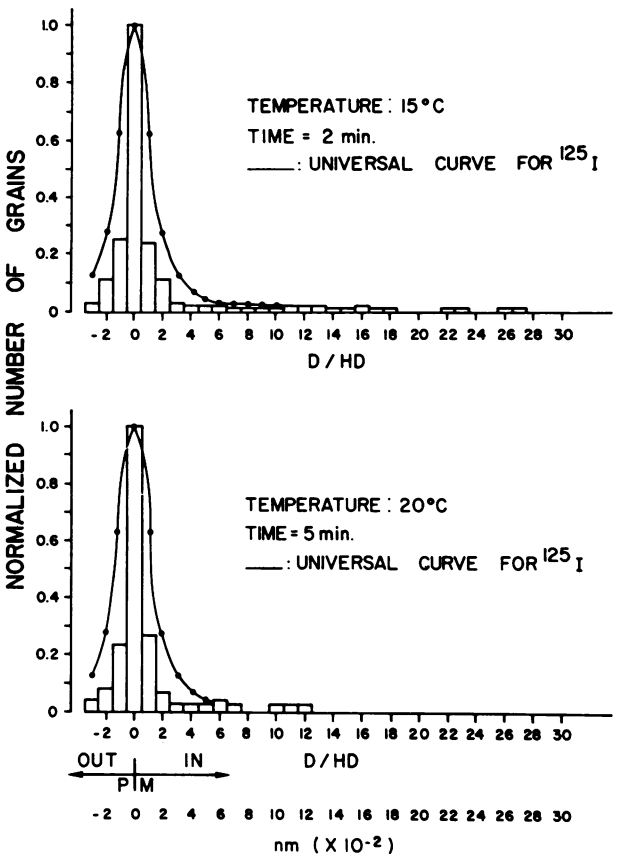

FIGURE 3 Distribution of ^{125}I-insulin around plasma membrane of IM-9 cultured human lymphocytes (top) and distribution of ^{125}I-glucagon in isolated rat hepatocytes (bottom). The methods of binding, preparation for autoradiography, and analysis of data for the hepatocytes were similar to the methods used for the lymphocyte previously described (12). In this analysis, the normalized number of grains was plotted as a function of the distance of the grain center to the plasma membrane, and the histogram was constructed therefrom. This distance was expressed both in nanometers and in half-distance (distance from a line source of ^{125}I that contains 50% of the developed grains). This last unit is used only for comparison with the universal curve of ^{125}I irradiation. The solid line represents the universal curve of ^{125}I irradiation and is derived from the distribution of ^{125}I irradiation around a defined line source (13). We have previously established that when ^{125}I-insulin is incubated with human lymphocytes for 2 min at 15°C (12) and with isolated hepatocytes for 5 min at 20°C (8), the distribution of autoradiographic grains is consistent with localization to plasma membrane. Similarly, when isolated rat hepatocytes are incubated with labeled glucagon for 5 min at 20°C, the distribution of autoradiographic grains is consistent with predominant plasma membrane localization.

^{125}I-glucagon with isolated hepatocytes. We have assumed in this and previous studies that the incubation of labeled hormones at low temperatures for short periods of time most closely simulates the initial binding step. When ^{125}I-glucagon is incubated with isolated hepatocytes for 5 min at 20°C, developed grains are easily detected at the cell periphery. When a large number of grains are photographed and their distribution analyzed by the method of Salpeter et al. (13), it can be seen that grains distribute symmetrically around the plasma membrane (Fig. 3). This distribution is essentially identical to the binding of ^{125}I-insulin to cultured human lymphocytes and isolated rat hepatocytes; in addition, this grain distribution fits within the universal curve of ^{125}I irradiation from a defined line source (Fig. 3).

Thus, ^{125}I-glucagon initially localizes to the plasma membrane. To determine whether grains localize to specialized regions of the plasma membrane such as coated invaginations, we have evaluated 200 photographs in which grains appear ±250 nm of the plasma membrane. Although coated invaginations are easily detected, <1% of the grains analyzed were found associated with these structures (data not shown).

Quantitative studies of apparent steady-state binding. When hepatocytes are incubated with 0.7 nM ^{125}I-glucagon at 20°C, the labeled material progressively associates with the cell up until 90 min, when apparent steady-state binding is reached and maintained for at least 120 min (Fig. 4). In three of the four experiments shown in Table I, there is little shift in grain distribution over the entire incubation period, but in one experiment a moderate grain shift is observed at later times of incubation (Fig. 5) (Table I).

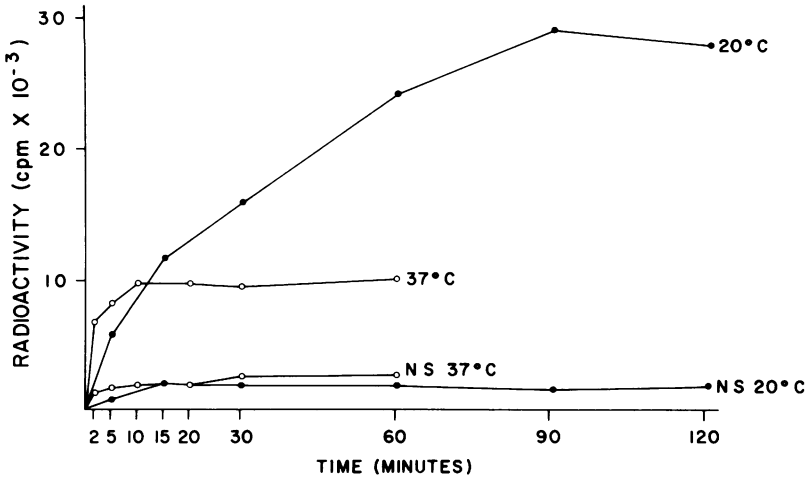

FIGURE 4 Time-course binding of 0.7 nM ^{125}I-glucagon to isolated rat hepatocytes at 20° (experiment 1) and 37°C (experiment 2). At 20°C, steady-state binding is reached by 90 min, whereas at 37°C, a steady state is achieved in 10–20 min. Nonspecific (NS) binding is low at both temperatures used.

In contrast to the 20°C experiments, when cells are incubated at 37°C, steady-state binding is reached by 10 min of incubation and maintained for at least 60 min (Fig. 4). By 30 min of incubation there is significant translocation of ^{125}I-glucagon, as demonstrated by the grain-distribution histogram (Fig. 6). When all four

TABLE I
Characteristics of Cell-associated Radioactivity from Cells Incubated at 20°C

Experiment		Time (min)					
		5	15	30	60	90	120
1	Percent translocated*	0	0	1	1	0	1
	Total number of grains analyzed	82	96	130	141	135	182
	Percent total ^{125}I-glucagon bound‡	1.12	2.45	3.44	4.94	5.96	5.74
	Percent total ^{125}I-glucagon nonspecifically bound	0.09	0.25	0.31	0.34	0.27	0.39
2	Percent translocated*	0	0	19	18	16	31
	Total number of grains analyzed	156	115	114	140	147	127
	Percent total ^{125}I-glucagon bound‡	1.30	2.17	3.56	4.44	4.21	4.58
	Percent total ^{125}I-glucagon nonspecifically bound	0.29	0.29	0.33	0.38	0.38	0.50
3	Percent translocated*	0	—	—	—	5	7
	Total number of grains analyzed	171	—	—	—	155	180
	Percent total ^{125}I-glucagon bound‡	2.56	—	—	—	6.64	7.57
	Percent total ^{125}I-glucagon nonspecifically bound	0.32	—	—	—	0.46	0.47
4	Percent translocated*	0	—	4	—	—	5
	Total number of grains analyzed	86	—	121	—	—	160
	Percent total ^{125}I-glucagon bound‡	5.22	—	2.11	—	—	11.22
	Percent total ^{125}I-glucagon nonspecifically bound	2.65	—	2.31	—	—	2.55

* To calculate the percent translocation for each experiment, the 5-min time point at 20°C was used as a control. For example, in the first experiment, 87% of grains were contained within ±250 μm. For each time point, the percent translocation is therefore the percent grains beyond 250 μm minus 13%.

$$\text{Percent translocation} = \left(\frac{\text{grains} > 250\ \mu\text{m}}{\text{total grains}} - 0.13\right) \times 100.$$

‡ Approximate counts per minute bound for each time point can be calculated for both total and nonspecific by taking 5×10^5 cpm for ^{125}I-glucagon.

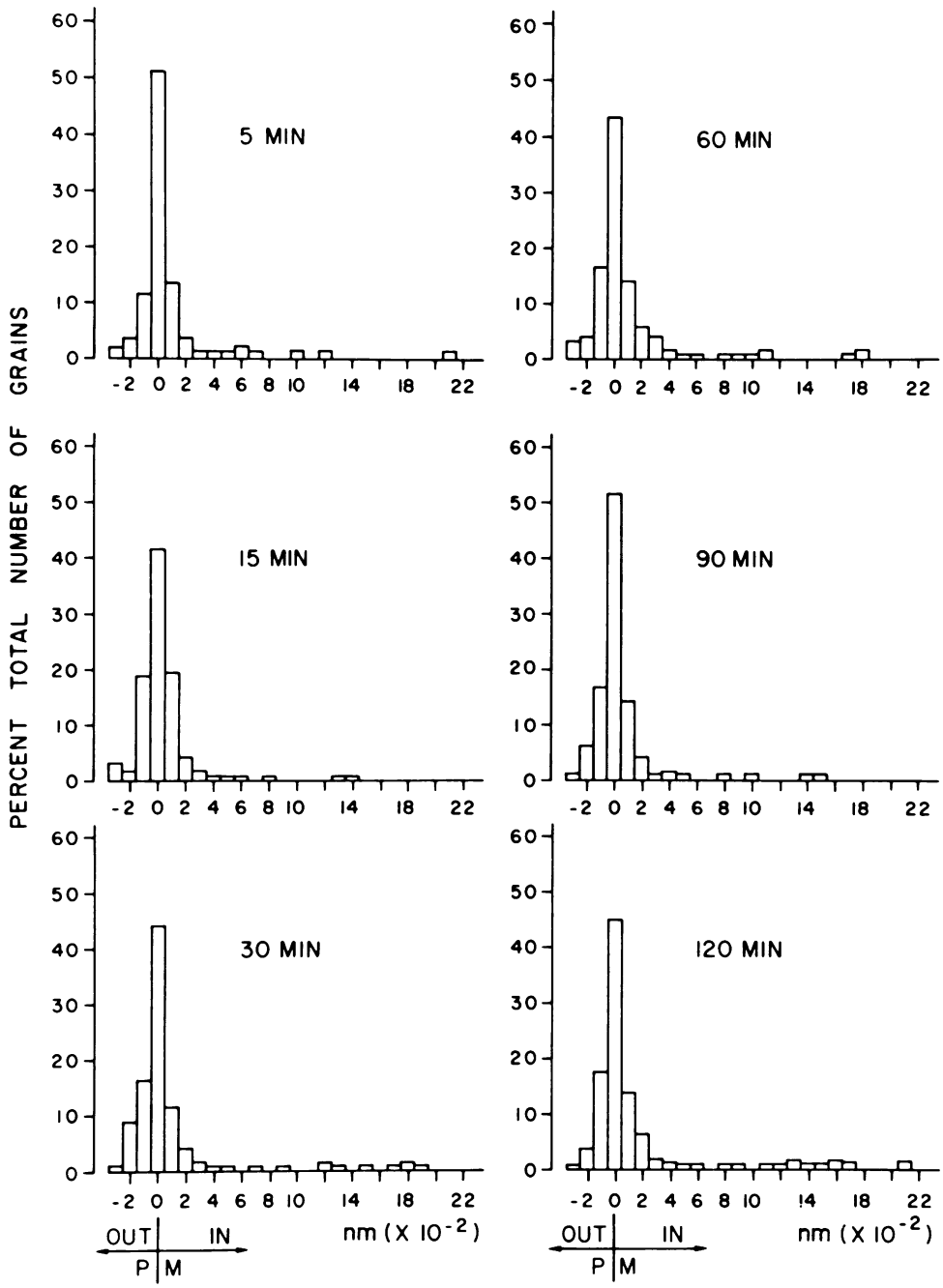

FIGURE 5 Grain-distribution histogram of ^{125}I-glucagon binding to isolated hepatocytes after incubation with 0.7 μM ^{125}I-glucagon at 20°C (experiment 1). The percent total number of grains was plotted as a function of the distance of the grain center to the plasma membrane, and histograms were constructed therefrom. In this experiment, there was essentially no change in autoradiographic grains distribution from 5 to 20 min; this is consistent with plasma membrane localization of grains. For further details of this experiment, see experiment 1, Table I.

incubations are considered for 30- and 60-min time periods, a mean of 30% of the labeled glucagon is internalized by the cell, and the remainder is localized to the plasma membrane (Table II).

Since autoradiography measures total binding, we wished to be certain that nonspecific binding (cell-associated radioactivity in the presence of excess unlabeled glucagon) did not significantly influence

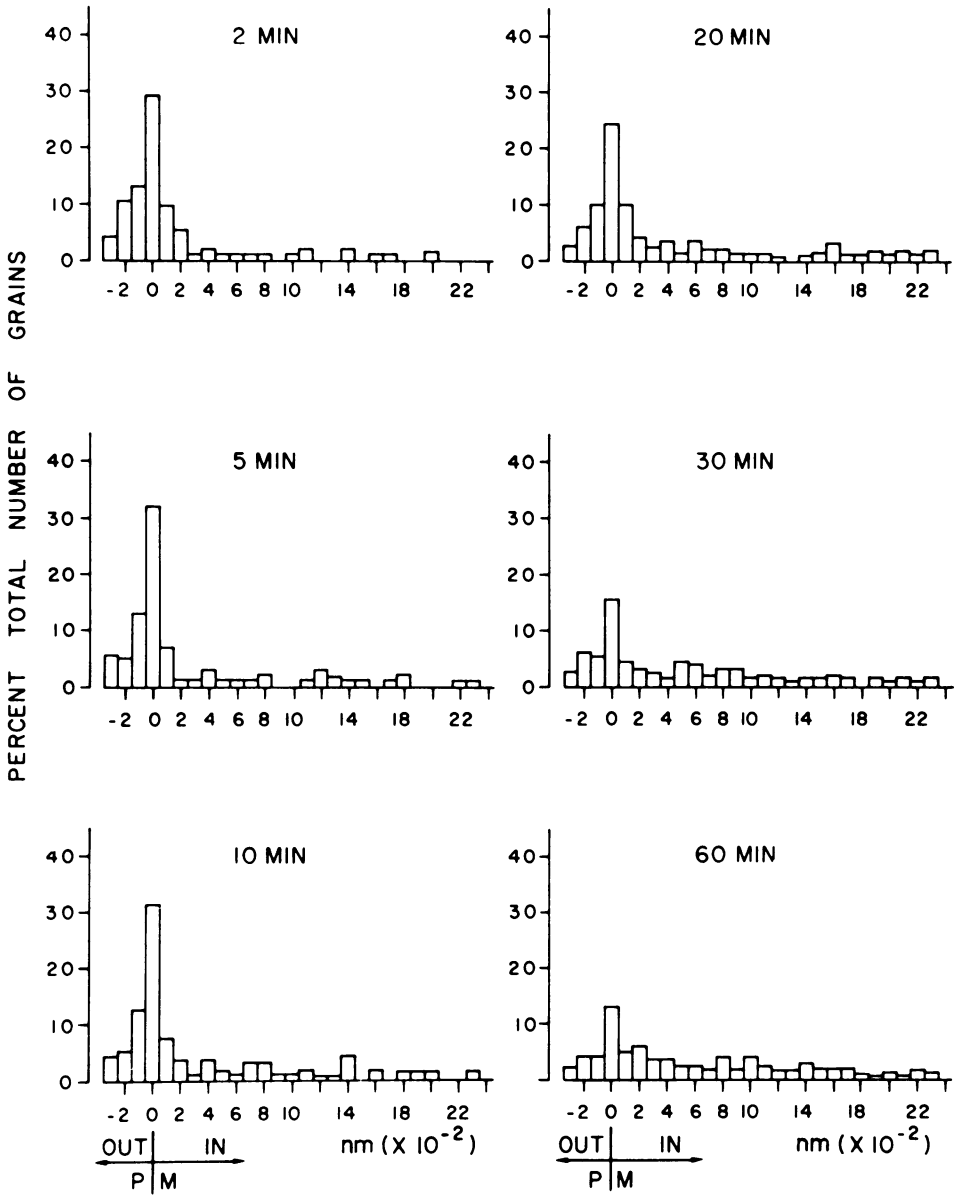

FIGURE 6 Grain-distribution histogram of ^{125}I-glucagon binding to isolated hepatocytes at 37°C (experiment 2). Histograms corresponding to each time point of binding analyzed were constructed as in Fig. 4. At the initial time of incubation, most grains localized to the plasma membrane, but with increasing time of incubation there was a progressive shift of the grains to an intracellular compartment extending to a maximal distance of ~1,700 nm. Data were derived from Table II.

total grain distribution. First, it can be seen that nonspecific binding is a relatively small proportion of the total binding at both 20° and 37°C (Fig. 4) (Tables I and II). Further, it can be seen that the nonspecific binding distributes in the same way as the total binding and therefore has little influence on the interpretation of the shift in grain distribution as a function of time (Fig. 7).

Quantitative localization of internalized ^{125}I-glucagon. To determine whether internalized grains preferentially localize to specific intracellular structures, we have measured the volumetric density of the major intracellular organelles of the peripheral (2 μm) cytoplasm, in which grains predominantly localize, and have previously reported these data in detail (6). We next used a probability circle method to estimate the probability that a given structure represents the source of a developed grain. The

TABLE II

Characteristics of Cell-associated Radioactivity from Cells Incubated at 37°C

Experiment		Time (min)					
		2	5	10	20	30	60
1	Percent translocated*	4	4	6	13	17	29
	Total number of grains analyzed	46	195	136	181	180	157
	Percent total ^{125}I-glucagon bound‡	1.29	1.88	2.02	2.54	2.72	2.49
	Percent total ^{125}I-glucagon nonspecifically bound	0.26	0.29	0.14	0.17	0.22	0.35
2	Percent translocated*	1	3	3	11	30	33
	Total number of grains analyzed	117	100	130	125	193	160
	Percent total ^{125}I-glucagon bound‡	1.32	1.65	2	1.90	1.85	2
	Percent total ^{125}I-glucagon nonspecifically bound	0.27	0.27	0.31	0.34	0.44	0.45
3	Percent translocated*	12	—	—	—	34	38
	Total number of grains analyzed	134	—	—	—	166	174
	Percent total ^{125}I-glucagon bound‡	1.77	—	—	—	2.32	2.41
	Percent total ^{125}I-glucagon nonspecifically bound	0.24	—	—	—	0.40	0.46
4	Percent translocated*	8	—	12	—	28	36
	Total number of grains analyzed	182	—	168	—	134	137
	Percent total ^{125}I-glucagon bound‡	4.88	—	5.27	—	6.14	5
	Percent total ^{125}I-glucagon nonspecifically bound	2.13	—	1.86	—	1.77	2

* For the method of calculation see Table I.

‡ Approximate counts per minute bound for each time point can be calculated for both total and nonspecific by taking 5×10^5 cpm for ^{125}I-glucagon.

analysis was restricted to grains beyond 250 nm of the plasma membrane.

When the percentage of grains associated with a given structure was expressed in terms of the volume density of the structure, it can be seen that there is a fivefold preferential association of grains to lysosome-like structures (Figs. 8 and 9), whereas there is no preferential association to mitochondria, microbodies, rough endoplasmic reticulum, or glycogen (nucleus and lipid droplets, not shown, are associated with <1% of grains). Examples of membrane-bounded structures considered lysosomelike are shown in Fig. 8.

Nature of the cell-associated radioactivity. Morphologically intact, biologically active, freshly isolated hepatocytes release soluble protease activity into their incubation media (Figs. 1 and 2). When cells are incubated for 30–60 min at 37°C and separated from the incubation media, the media activity degrades labeled glucagon and insulin. To study cell-related degradation, it is first necessary to inhibit this soluble protease activity. Bacitracin inhibits this activity by about 85% over a 1-h incubation at 37°C, and we have included this protease inhibitor in all incubations. We have previously shown that bacitracin does not inhibit internalization[2] (6, 8), and this has recently been confirmed (22). Ammonium chloride inhibits cell-related degradation as shown below, but has no affect on the soluble protease activity.

When cells are incubated with labeled glucagon and washed, and the cell-associated radioactivity is extracted and filtered on G-50 Sephadex, the radioactivity elutes predominantly in two peaks. The major peak elutes coincident with the ^{125}I-glucagon marker, and the other peak elutes beyond the ^{125}I elution volume in the region of iodotyrosyle peptides (Fig. 10). A small, relatively constant peak is seen in the void region of the column. For incubations carried out at 20°C, most of the radioactivity elutes in the position of glucagon, up until 120 min (Fig. 11, right). For incubations carried out at 37°C, there is a greater and progressive decrease in radioactivity eluting as intact glucagon, up until 60 min of incubation (Fig. 11, left). When the radioactivity appearing in the incubation media is analyzed at each time point of incubation at both 20° and 37°C, the data is generally similar to what is seen in the cell extracts (Tables III and IV). We have previously found that degraded products are not taken up by the cells and are largely lost from the hepatocytes during the processing of the pellet (6). Thus, most of the radioactivity that was recorded in our autoradiogram was derived from material with a molecular size similar to native glucagon. These data are similar to what we have previously reported for insulin in the hepatocyte (6).

[2] Receptor-linked ^{125}I-insulin degradation is mediated by internalization. Manuscript submitted for publication.

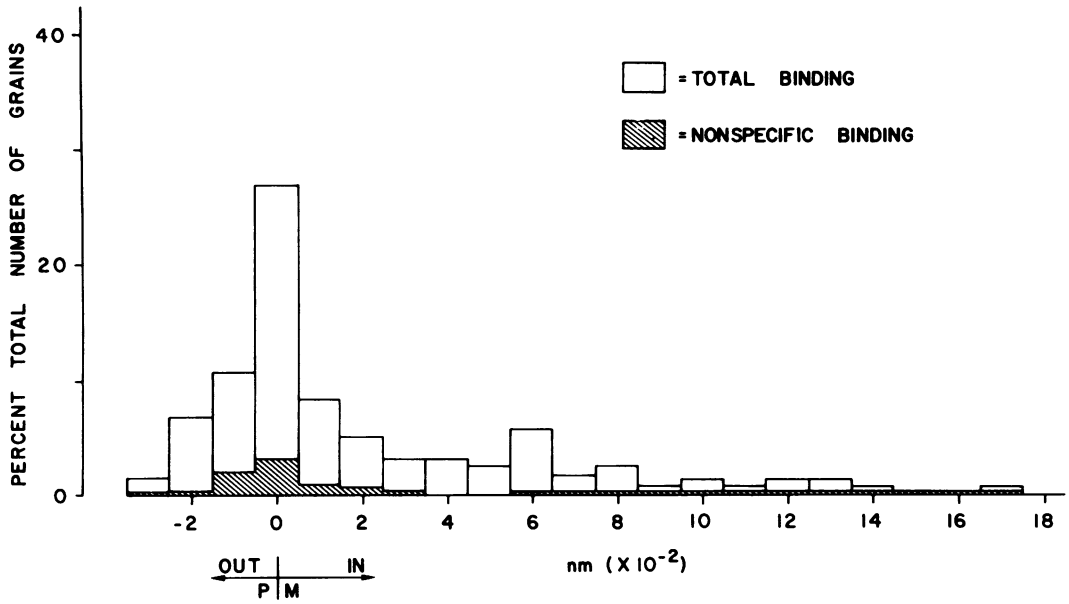

FIGURE 7 Grain-distribution histogram of ^{125}I-glucagon binding to isolated hepatocytes after 60 min of incubation with 0.7 nM ^{125}I-glucagon at 37°C. The open columns represent the distribution of grains corresponding to total binding. The percentage of total number of grains is plotted as a function of the distance of grain center to the plasma membrane. In this condition, 60% of the grains distribute around the plasma membrane, and 40% are found inside the cell. Biochemical data indicate that in this experiment, nonspecific binding represented 14% of the total binding. To know whether this nonspecific component could influence the total binding grain distribution, we compared grain-distribution histograms of total and nonspecific binding for identical time and temperature of incubation (60 min at 37°C). This analysis showed clearly that nonspecific binding distributes in the same way as the total binding and cannot be responsible for the shift in grain distribution observed for total binding.

To determine the relationship between the proportion of the ligand internalized and the proportion of the ligand degraded, the mean value of the percent ^{125}I-glucagon internalized at each time point for the four incubations shown in Table II was plotted as a function of the percent ^{125}I-glucagon degraded (Fig. 11); a strong positive correlation between these two parameters was found ($r = 0.95$).

In an additional experiment, hepatocytes were incubated for 60 min with the lysosomal stabilizing

TABLE III
Analysis of Media Radioactivity of ^{125}I-Glucagon Incubated with Isolated Hepatocytes at 20°C

	Time (min)			
	5	30	60	120
	%			
Elution peak II	87	86	85	83
Talc adsorption	96	95	93	91
Trichloracetic acid precipitation	87	79	71	62

In this experiment, an aliquot of the incubation media was taken at each time point shown and either analyzed by Sephadex gel filtration as shown in Fig. 10 or by talc adsorption and trichloracetic acid precipitation as previously described (23).

TABLE IV
Analysis of Media Radioactivity of ^{125}I-Glucagon Incubated with Isolated Hepatocytes at 37°C

	Time (min)			
	2	10	30	60
	%			
Elution peak II	90	90	88	82
Talc adsorption	96	95	90	86
Trichloracetic acid precipitation	83	77	62	38

In this experiment, an aliquot of the incubation media was taken at each time point shown and either analyzed by Sephadex gel filtration as shown in Fig. 10 or by talc adsorption and trichloracetic acid precipitation as previously described (23).

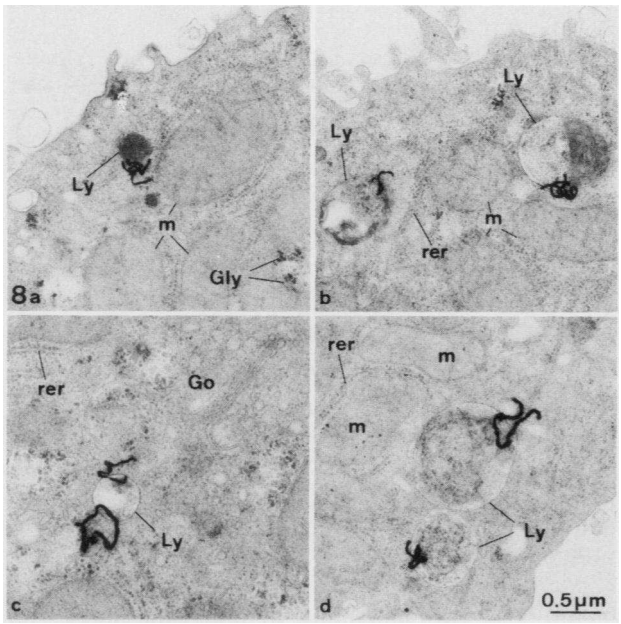

FIGURE 8 Selected images of developed autoradiographic grains associated with structures referred to as lysosomelike. These include autophagosomes (*b*, *d*); multivesicular bodies (*c*), dense bodies (*a*), and glycogenosomes (*b*). Ly, lysosomes; Gly, glycogen; m, mitochondria; rer, rough endoplasmic reticulum; Go, Golgi complex. ×22,000.

agent, 8 mM ammonium chloride. In this case there was less cell-related degradation than seen in incubations where only bacitracin was present (Table V).

DISCUSSION

We conclude from these studies that (*a*) at early time periods of incubation, labeled glucagon initially localizes to the plasma membrane of the hepatocyte; (*b*) at 20°C the labeled material remains predominantly localized to the plasma membrane from initial binding through apparent steady-state binding; (*c*) at 37°C, after a brief delay, the labeled material is progressively internalized by the hepatocyte; (*d*) the internalized labeled material preferentially associates with lysosomelike structures; (*e*) when ^{125}I-glucagon is incubated with hepatocytes at 37°C, the cell-associated radioactivity is degraded as a function of incubation time.

Thus, labeled glucagon interacts with the hepatocyte in a qualitatively similar fashion to labeled insulin. Both ligands initially bind to the plasma membrane; both ligands are internalized by the cell at 37°C; both ligands preferentially associate with lysosomal structures; and both ligands are degraded by the cell (6). Glucagon and insulin differ somewhat quantitatively in their interaction with the hepatocyte in that the internalization of glucagon is somewhat slower and more temperature dependent. The internalization of ^{125}I-insulin is proportional to binding at both 20° and 37°C, whereas the rate of internalization of ^{125}I-glucagon is more delayed with respect to the rate of binding (24). Inasmuch as the cell is the same in both cases, the differences must reside in the ligand or the specific receptor. It is unclear, however, what property is important in producing these differences.

When analyzed in an appropriate quantitative fashion, the EM autoradiographic technique is well suited to measuring ^{125}I radioactivity on the plasma membrane, and when a base line is established, a shift in grain distribution clearly indicates internalization of radioactivity (12, 13). We have shown that nonspecific binding and background irradiation do not

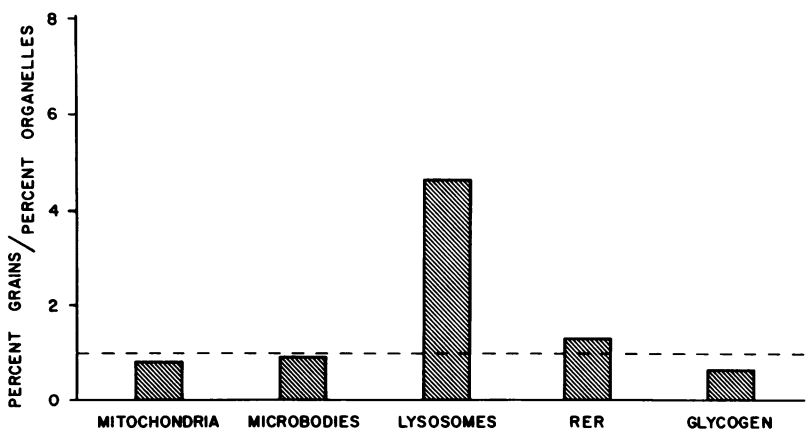

FIGURE 9 Relationship of autoradiographic grains to intracellular organelles (mitochondria, microbodies, lysosomes, rough endoplasmic reticulum, and glycogen) expressed as the ratio of the percentage of grains related to organelles over the relative volume occupied by intracytoplasmic organelles (volume density) (experiment 4).

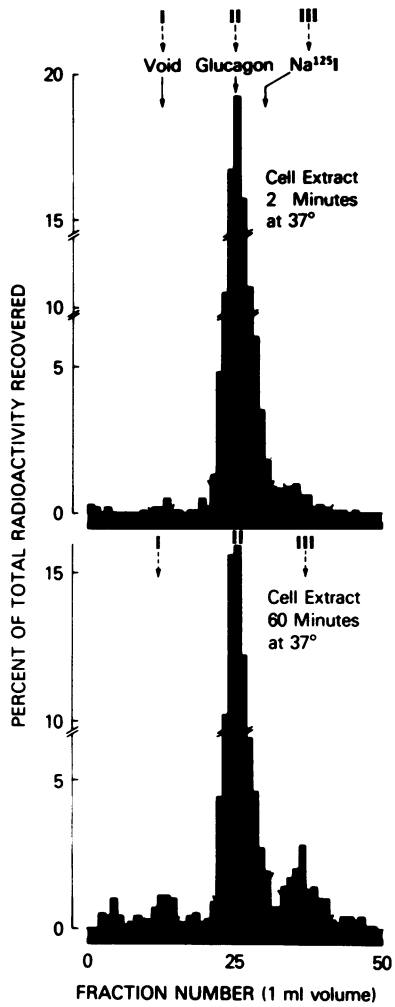

FIGURE 10 Sephadex G-50 filtration elution profile of extract of cell-associated radioactivity. Hepatocytes were incubated with ^{125}I-glucagon in Krebs-Ringer bicarbonate buffer in the presence of 0.8 mg/ml of bacitracin. At the end of each time point of incubation (shown in Figs. 5 and 6), cells were centrifuged and the pellet washed with buffer. The cell pellet was then extracted with a mixture of 0.1% Triton X-100, 3 M acetic acid, and 6 M urea, and the mixture centrifuged at 12,000g for 5 min. The supernate (87–97% of total cellular radioactivity) was then applied at a G-50 (fine) column (0.9 × 50 cm), which was either equilibrated in and eluted by the extraction mixture or by 1 M acetic acid. The peak elution volume of the void, ^{125}I-glucagon, and ^{125}I are shown at the top and the slashes designate the fractions (1 ml each) pooled for peaks I, II, and III. Peak I (void) refers to fraction 11–15; peak II (intact ^{125}I-glucagon) to fraction 22–32; and peak III (degraded products) to fraction 33–42. The results of all incubation times at 20° and 37°C are given in Fig. 11.

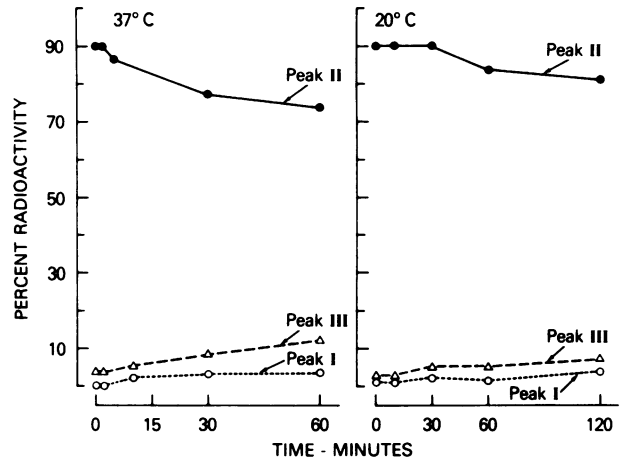

FIGURE 11 Percentage of radioactivity appearing in Sephadex elution profile shown in Fig. 10 for each time point of incubation.

account for the shifts in grain distribution. We have interpreted these data to mean that ^{125}I-glucagon initially binds to specific cell surface receptors and is internalized by adsorptive pinocytosis into small endocytic vesicles, and that these vesicles subsequently fuse with membrane-bounded structures with the morphologic characteristics of secondary lysosomes. As in our previous study with ^{125}I-insulin in the isolated hepatocyte, we have been unable quantitatively to associate labeled glucagon with structures having the morphologic characteristics of endocytic vesicles. We believe this is due to our inability to resolve these small structures quantitatively by the autoradiographic technique. Morphologic probes with higher resolution demonstrate both low density lipoprotein (25) and epidermal growth factor (26) in presumably endocytic vesicles at early times of incubation.

We have shown, however, that grains are preferentially localized to membrane-bounded structures, which we interpret to be secondary lysosomes. First, these structures are indistinguishable from our previous study with labeled insulin (cf. Fig. 9 with Fig. 3 of reference 6). In addition, when cytochemical techniques are used, we find, in preliminary studies, that grains frequently associate with acid phosphatase-

TABLE V

Sephadex G-50 Elution Profile of Radioactivity Extracted from Hepatocytes Incubated in the Presence or Absence of Ammonium Chloride for 60 min at 37°C

Condition	Elution		
	Peak I	Peak II	Peak III
		%	
Bacitracin	3	69	20
Bacitracin plus 8 mM ammonium chloride	2	83	9

Methods are the same as for experiments shown in Figs. 10 and 11.

positive structures.[3] Finally, we have applied the autoradiographic technique used in this study to five different ligands in four cell types: these include low density lipoprotein (27) and epidermal growth factor binding to cultured human fibroblast (28, 29); insulin binding to cultured human lymphocytes (12, 30), isolated rat hepatocytes (6), and intact liver (7); human growth hormone (31) and anti-insulin receptor antibodies to cultured human lymphocytes (32); and epidermal growth factor binding to human epidermoid carcinoma cells.[4] In addition, we have compared the autoradiographic technique to studies using ferritin-labeled ligands in two of these systems (27).[4] When these studies are taken together, they suggest that all of the ligands studied in the different cell types are involved in a similar qualitative process, and that all of these systems involve lysosomal association of the internalized material.

Our studies demonstrate the initial localization of ^{125}I-glucagon to the cell membrane by a morphologic technique. The data confirm previous biochemical studies and further suggest that binding, internalization, and lysosomal processing are general mechanisms related to many polypeptide hormones and growth factors.

Because all the components of the glucagon system necessary for the expression of a biologic effect (i.e., receptor-adenylate cyclase and its nucleotide-binding regulatory subunit) are contained in the plasma membrane, it is unlikely that internalization is necessary for the biologic action of glucagon. This assumption is further supported by the delay in internalization with respect to binding at physiologic temperatures.

There are at least two other functions mediated through the hormone receptor: these include degradation of the ligand (33) and the ability of the hormone to regulate the concentration of its cell surface receptor (34).

Recent studies have shown that hepatic metabolism accounts for 32% of the metabolic clearance rate for glucagon and 49% of the metabolic clearance rate of insulin (35). These figures are consistent with the relative proportions of glucagon (see Table II) and insulin (24) internalized by the hepatocyte under apparent steady-state conditions, and support the notion that one function of the internalization process is to remove the hormone from the cell surface to an internal degradation site.

Although we cannot conclude that the hepatocyte degrades glucagon exclusively by way of a lysosomal pathway, we have shown that glucagon degradation is occurring, as the incubation proceeds, in a similar fashion to that of labeled insulin (6, 8). In addition, both glucagon and insulin degradation in hepatocytes are inhibited by agents such as ammonium chloride (36), which are thought to act as lysosomal stabilizing agents.[5] The degradation of glucagon as insulin by hepatocytes is complex, involving both cell-related processes and soluble proteases. It is not possible, therefore, to quantify directly the lysosomal component of glucagon degradation.

It is now well established for a number of polypeptide hormones and growth factors that the ligand can cause the loss of its cell surface receptor. This process has been demonstrated for glucagon both in vivo (10, 38, 39) and in vitro (40). If internalization occurs by way of adsorptive pinocytosis, then the membrane segment containing the receptor may also be internalized (41). Under these conditions the specific hormone receptor would be lost from the cell surface. Since the various components of the receptor-effector system (the receptor and the catalytic subunits) are presumably free to move in the plane of the membrane, each component may be internalized separately.

Other polypeptide hormones that have similarities to glucagon, in that they act through a second messenger, appear to behave in a similar fashion to glucagon (42, 43).

The mechanism by which a presumed univalent ligand such as glucagon, other polypeptide hormones, and growth factors appear to induce their internalization by the cell is unknown. It is attractive to speculate that these agents induce some form of aggregation of their specific receptor proteins, but further work will be necessary to confirm these speculations.

ACKNOWLEDGMENTS

We are indebted to M. Sidler-Ansermet, O. Jerotic, N. Grenier-Brossette, and P. A. Rüttiman for skilled technical assistance.

This investigation was supported by grant 3.120.77 from the Swiss National Science Foundation and by grant 77.7.0247 from the Délégation Générale à la Récherche Scientifique et Technique (France).

REFERENCES

1. Exton, J. M., and C. R. Park. 1968. The role of cyclic AMP in the control of liver metabolism. *Adv. Enzyme Regul.* **6**: 391–407.

[3] In preliminary studies we find that when ^{125}I-insulin is incubated with isolated hepatocytes and ^{125}I-human growth hormone is incubated with cultured human lymphocytes, that approximately one-third and one-half, respectively, of lysosomelike structures associated with grains are positive for a single lysosomal marker (acid phosphatase). These values are somewhat higher than reported by Bergeron et al. (5), as previously discussed (7).

[4] We have studied by our autoradiographic technique cells of the A-431 epidermoid carcinoma line that have previously been studied for ferritin-epidermal growth factor binding by Haigler et al. (26).

[5] For additional discussion of lysosomal degradation and lysosomal stabilizing agents, see Reference 37.

2. Rodbell, M. 1972. Regulation of glucagon action on its receptors. *In* Glucagon: Molecular Physiology, Clinical and Therapeutic Implications. P. J. Lefebvre and R. H. Unger, editors. Pergamon Press. 61–75.
3. Sutherland, E. W., G. A. Robison, and R. W. Butcher. 1968. Some aspects of the biological role of adenosine 3′,5′-monophosphate (cyclic AMP). *Circulation.* **37:** 279–306.
4. Bergeron, J. J. M., G. Levine, R. Sikstrom, D. O'Shaughnessy, B. Kopriwa, N. J. Nadler, and B. I. Posner. 1977. Polypeptide hormone binding "in vivo": initial localization of ^{125}I-labeled insulin to hepatocyte plasmalemma as visualized by electron microscope radioautography. *Proc. Natl. Acad. Sci. U.S.A.* **74:** 5051–5055.
5. Bergeron, J. J. M., R. Sikstrom, A. R. Hand, and B. I. Posner. 1979. Binding and uptake of ^{125}I-insulin into rat liver hepatocytes and endothelium: an in vivo radioautographic study. *J. Cell Biol.* **80:** 427–443.
6. Carpentier, J-L., P. Gorden, P. Freychet, A. LeCam, and L. Orci. 1979. Lysosomal association of internalized ^{125}I-insulin in isolated rat hepatocytes: direct demonstration by quantitative electron microscopic autoradiography. *J. Clin. Invest.* **63:** 1249–1261.
7. Carpentier, J-L., P. Gorden, P. Barazzone, P. Freychet, A. LeCam, and L. Orci. 1979. Intracellular localization of ^{125}I-insulin in hepatocytes from intact rat liver. *Proc. Natl. Acad. Sci. U.S.A.* **76:** 2803–2807.
8. Gorden, P., J-L. Carpentier, P. Freychet, A. LeCam, and L. Orci. 1978. Intracellular translocation of iodine-125-labeled insulin: direct demonstration in isolated hepatocytes. *Science (Wash. D. C.).* **200:** 782–785.
9. Seglen, P. O. 1976. Preparation of isolated rat liver cells. *Methods Cell Biol.* **13:** 79–83.
10. Fouchereau-Peron, M., F. Rancon, P. Freychet, and G. Rosselin. 1976. Effect of feeding and fasting on the early steps of glucagon action in isolated rat liver cells. *Endocrinology.* **98:** 755–760.
11. Caro, L. G., R. P. Van Tubberghen, and J. A. Roll. 1962. High resolution autoradiography. I. Methods. *J. Cell Biol.* **15:** 173–188.
12. Carpentier, J-L., P. Gorden, M. Amherdt, E. Van Obberghen, C. R. Kahn, and L. Orci. 1978. ^{125}I-insulin binding to cultured human lymphocytes: initial localization and fate of hormone determined by quantitative electron microscopic autoradiography. *J. Clin. Invest.* **61:** 1057–1070.
13. Salpeter, M. M., H. C. Fertuck, and E. E. Salpeter. 1977. Resolution in electron microscope autoradiography. III. Iodine-125, the effect of heavy metal staining, and a reassessment of critical parameters. *J. Cell Biol.* **72:** 161–173.
14. Staübli, W., W. Schweizer, J. Suter, and E. R. Weibel. 1977. The proliferative response of hepatic peroxisomes of neonatal rats to treatment with SU-13 437 (nafenopin). *J. Cell Biol.* **74:** 665–689.
15. Drochmans, P., J-C. Wanson, and R. Mosselmans. 1975. Isolation and subfractionation of Ficoll gradients of adult rat hepatocytes: size, morphology, and biochemical characteristics of cell fractions. *J. Cell Biol.* **66:** 1–22.
16. LeCam, A., A. Guillouzo, and P. Freychet. 1976. Ultrastructural and biochemical studies of isolated adult rat hepatocytes prepared under hypoxic conditions. *Exp. Cell Res.* **98:** 382–395.
17. LeCam, A., and P. Freychet. 1978. Effect of catecholamines on amino acid transport in isolated rat hepatocytes. *Endocrinology.* **102:** 379–385.
18. Freychet, P., and A. LeCam. 1978. Amino acid transport in isolated hepatocytes: effect of glucagon. *In* Hepatotrophic Factors. Ciba Foundation Symposium. Excerpta Medica, Amsterdam. **55**(N.S.): 247–268.
19. LeCam, A., and P. Freychet. 1976. Glucagon stimulates the A system for neural amino acid transport in isolated hepatocytes of adult rat. *Biochem. Biophys. Res. Commun.* **72:** 893–901.
20. LeCam, A., and P. Freychet. 1977. Effect of glucocorticoids on amino acid transport in isolated rat hepatocytes. *Mol. Cell. Endocr.* **9:** 205–214.
21. LeCam, A., and P. Freychet. 1978. Effect of insulin on amino acid transport in isolated rat hepatocytes. *Diabetologia.* **15:** 117–123.
22. Haigler, H. T., M. C. Willingham, and I. Pastan. 1980. Inhibitors of ^{125}I-epidermal growth factor internalization. *Biochem. Biophys. Res. Commun.* **94:** 630–637.
23. Freychet, P., R. Kahn, J. Roth, and D. M. Neville, Jr. 1972. Insulin interactions with liver membranes: independence of binding of the hormone and its degradation. *J. Biol. Chem.* **247:** 3953–3961.
24. Carpentier, J-L., P. Gorden, P. Freychet, A. LeCam, and L. Orci. 1979. Relationship of binding to internalization of ^{125}I-insulin in isolated rat hepatocytes. *Diabetologia.* **17:** 379–384.
25. Anderson, R. G. W., M. S. Brown, and J. L. Goldstein. 1977. Role of the coated endocytotic vesicle in the uptake of receptor-bound low density lipoprotein in human fibroblasts. *Cell.* **10:** 351–364.
26. Haigler, H. T., J. A. McKanna, and S. Cohen. 1979. Direct visualization of the binding and internalization of a ferritin conjugate of epidermal growth factor in human carcinoma cells A-431. *J. Cell Biol.* **81:** 382–395.
27. Carpentier, J-L., P. Gorden, J. L. Goldstein, R. G. W. Anderson, M. S. Brown, and L. Orci. 1979. Binding and internalization of ^{125}I-LDL in normal and mutant human fibroblasts: a quantitative autoradiographic study. *Exp. Cell Res.* **121:** 135–142.
28. Gorden, P., J-L. Carpentier, S. Cohen, and L. Orci. 1978. Epidermal growth factor: morphological demonstration of binding, internalization, and lysosomal association in human fibroblasts. *Proc. Natl. Acad. Sci. U.S.A.* **75:** 5025–5029.
29. Gorden, P., J-L. Carpentier, S. Cohen, and L. Orci. 1978. Interaction du facteur de croissance épidermique avec des fibroblastes humains en culture: une étude autoradiographique à l'échelon ultrastructural. *C. R. Acad. Sci. (Series D).* **286:** 1471–1474.
30. Gorden, P., J-L. Carpentier, E. Van Obberghen, P. Barazzone, J. Roth, and L. Orci. 1979. Insulin-induced receptor loss in the cultured human lymphocyte: quantitative morphological perturbations in the cell and plasma membrane. *J. Cell Sci.* **39:** 77–88.
31. Carpentier, J-L., M. A. Lesniak, P. Barazzone, E. Van Obberghen, P. Gorden, and L. Orci. 1979. Direct demonstration of binding and internalization of ^{125}I-hGH in cultured human lymphocytes: a mechanism linking degradation of the hormone with down regulation of the receptor. Proceedings of the 61st Annual Meeting Endocrine Society, Anaheim, Calif., June 1979. Abstract 30:80.
32. Carpentier, J-L., E. Van Obberghen, P. Gorden, and L. Orci. 1979. ^{125}I-Anti-insulin receptor antibody binding to cultured human lymphocytes: morphological events are similar to the binding of ^{125}I-insulin. *Diabetes.* **28:** 345. (Abstr.)
33. Terris, S., and D. Steiner. 1975. Binding and degradation of ^{125}I-insulin by rat hepatocytes. *J. Biol. Chem.* **250:** 8389–8398.
34. Gavin, J. R., III, J. Roth, D. M. Neville, Jr., P. De Meyts,

and D. N. Buell. 1974. Insulin-dependent regulation of insulin receptor concentrations: a direct demonstration in cell culture. *Proc. Natl. Acad. Sci. U.S.A.* **71:** 84–88.
35. Jaspan, J., K. Polonsky, M. Lewis, W. Pugh, J. Pensler, and A. Moossa. 1979. Hepatic metabolism (HM) of exogenous glucagon in the dog. *Diabetes.* **28:** 357. (Abstr.)
36. Gorden, P., J-L. Carpentier, P. Freychet, and L. Orci. 1979. Receptor linked ^{125}I-insulin degradation is mediated by internalization. *Clin. Res.* **27:** 485. (Abstr.)
37. Gorden, P., J-L. Carpentier, P. Freychet, and L. Orci. 1980. Internalization of polypeptide hormones: mechanism, intracellular localization and significance. *Diabetologia.* **18:** 1–12.
38. Srikant, C. B., D. Freeman, K. McCorkel, and R. H. Unger. 1977. Binding and biologic activity of glucagon in liver cell membranes of chronically hyperglucagonic rats. *J. Biol. Chem.* **252:** 7434–7436.
39. Bhathena, S. J., N. R. Voyles, S. Smith, and L. Recant. 1978. Decreased glucagon receptors in diabetic rat hepatocytes. *J. Clin. Invest.* **61:** 1488–1497.
40. Soman, V., and F. Felig. 1977. Glucagon receptor: "down regulation" by physiologic hyperglucagonemia. *Clin. Res.* **25:** 665. (Abstr.)
41. Silverstein, S. C., R. M. Steinman, and Z. A. Cohn. 1977. Endocytosis. *Annu. Rev. Biochem.* **46:** 669–722.
42. Amsterdam, A., A. Nimrod, S. A. Lamprecht, Y. Burstein, and H. R. Lindner. 1979. Internalization and degradation of receptor-bound hCG in granulosa cell cultures. *Am. J. Physiol.* **236:** E124–E138.
43. Chen, T. T., J. H. Abel, Jr., M. I. McCellan, H. R. Sawyer, M. A. Diekman, and G. D. Niswender. 1977. Localization of gonadotropic hormones in lysosomes of ovine luteal cells. *Cytobiologie.* **14:** 412–420.